19th Brazilian Congress of Thermal Sciences and Engineering
November 06th-10th, 2022, Bento Gonçalves - RS - Brazthe

ENC-2022-0129
MINIMIZATION OF ELECTRICITY GENERATION COSTS WITH SMALL CAPACITIES CC-MCI-CRO

Claudio Jose da Silva
Pontifical Catholic University of Minas Gerais, Department of Mechanical Engineering 500 dom José Gaspar Avenue, Belo Horizonte, MG, 30.535-901, BRAZIL
cjsilva@sga.pucminas.br

Alexander Valadares Weimann
Pontifical Catholic University of Minas Gerais, Department of Mechanical Engineering 500 dom José Gaspar Avenue, Belo Horizonte, MG, 30.535-901, BRAZIL
alexander.v.w@hotmail.com

Leonardo Silva Oliveira
Pontifical Catholic University of Minas Gerais, Department of Mechanical Engineering 500 dom José Gaspar Avenue, Belo Horizonte, MG, 30.535-901, BRAZIL
leonardosl2198@gmail.com

Marcos Araujo Lima
Pontifical Catholic University of Minas Gerais, Department of Mechanical Engineering 500 dom José Gaspar Avenue, Belo Horizonte, MG, 30.535-901, BRAZIL
Marcosalp1998@gmail.com

Felipe Raul Ponce Arrieta
Pontifical Catholic University of Minas Gerais, Department of Mechanical Engineering, 500 dom José Gaspar Avenue, Belo Horizonte, MG, 30.535-901, BRAZIL
IBMEC - Belo Horizonte, 300 Rio Grande do Norte Street, Employees, Belo Horizonte, MG, 30.130-130, BRAZIL
Felipe.ponce@pucminas.br

Abstract.
The possibility of waste heat recovery from internal combustion engines (ICM) must be studied and evaluated, as it results in excellent economic gains and environmental improvements. In this article we will estimate the waste heat recovery potential of the MCI, reaching the lowest cost of electricity production. Considering the energy available in the exhaust gases and coolant, we used a Wartsila 46DF, 4 stroke engine, with 10.3 MW of power. The study was developed through the steps Definition of the thermal cycle, Modeling the thermal cycle, and Waste heat recovery optimization. The organic Rankine cycle was chosen with two regenerative transcritical pressure levels, using Cyclopentane as working fluid. The cycle was modeled in Engineering Equation Solver (EES). The modeling included mass, energy, entropy and exergy balances by component and the cycle as a whole. The influence of cycle variables on performance and cost parameters was evaluated. The optimization was performed using the method of genetic algorithms available in EES. The best configuration for the organic Rankine cycle shown 1,020 kW, 17.65 % and 3,026 R$/kW for net power, thermal efficiency, and specific investment cost respectively.

Keywords: Organic Rankine cycle, Waste heat recovery, Electricity generation, Optimization, Cost, Internal combustion engines.

1. INTRODUCTION

The use of organic Rankine cycles (ORC) for electricity generation through the waste heat recovery in energy efficiency projects has become a reality and has been applied in several segments worldwide, as presented by Mahmoudi, Fazli and Morad (2018).

According to Heywood (2018), considering a typical internal combustion engine, more than 40% of the fuel energy is dissipated through exhaust gases and the cooling system. We will define an ORC for waste heat recovery in exhaust gases and cooling system, then we will perform the thermodynamic modeling of the cycle and develop a computational code in the EES software for its simulation. So, we can optimize the ORC to achieve the lowest specific electricity generation cost, Chatzopoulo (2018). By optimizing the ORC was maximized the specific investment cost considering the waste heat recovery efficiency.

2. METHODOLOGY

The ORC has been shown to be a promising solution when applied for waste heat recovery from internal combustion engines. The thermal efficiency of an ORC depends on the thermodynamic properties of the working fluid and the operating conditions of the exhaust gas, cooling system, and cycle thermal efficiency. Studies developed by Pinnau (2008), Rathod (2017) and Xu (2018) show that the average thermal efficiency of an ORC is range from 2 % to 19 %.

The ORC with two pressure levels is an improvement that has been developed to operate with two different kind of heat sources. This cycle adopts a high-pressure level responsible for waste heat recovery from a high temperature source and a low-pressure level responsible for waste heat recovery from a low temperature source. Thus, it is possible to obtain a waste heat recovery in the system because it allows the working fluid to have temperatures close to those of the sources during its evaporation.

2.1 Definition of the thermal cycle

Many works, such as those of Song et al. (201 5) concluded that, considering simple ORC for waste heat recovery from different heat sources, it is possible to take advantage of only a fraction of the energy dissipated by the lower temperature source. Considering the particularity of dissipated heat recovery in two distinct thermal sources of an MCI (exhaust gas and cooling system) it was decided to set ORC with two levels of regenerative transcritical pressure. Figure 1 demonstrates the thermal schematic representation of an ORC of two levels of regenerative transcritical pressure and its T-s diagram.

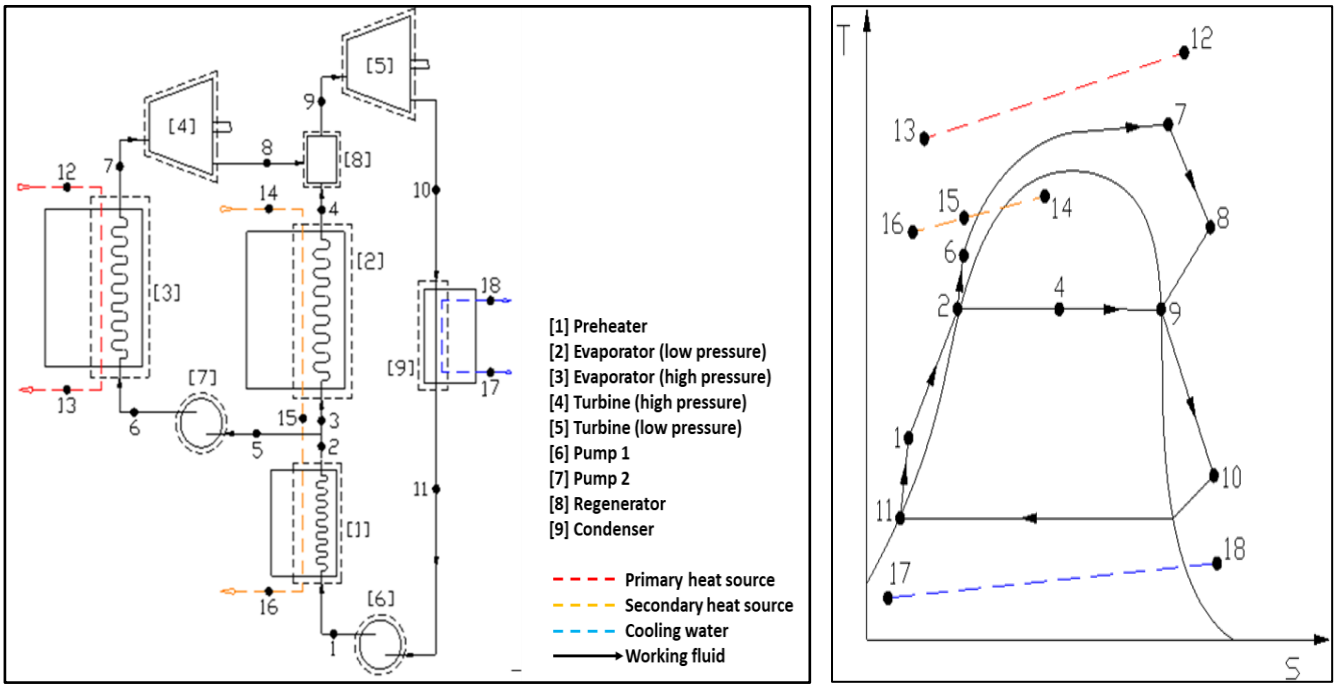

Figure 1: Representation of the chosen CRO and its T-s diagram.

The system features a high-pressure evaporator and a low-pressure evaporator, a preheater, a regenerator, a high-pressure pump and a low-pressure pump, a two-stage turbine, and a condenser. Evaporators [3] and [2] recover thermal energy from exhaust gases and cooling system respectively. The working fluid is pressurized by the pump [6], which passes through the preheater [1], and goes to the evaporator [2]. The pump [7] pressurizes part of the fluid to a supercritical pressure (process 5-6). The fluid absorbs thermal energy from the MCI exhaust gases through the evaporator [3], supercritical steam (process 6-7). This steam is then expanded and passes through the first stage (process 7-8) of the turbine [4]. The steam comes out of the turbine [4] and reaches the regenerator [8] and mixes with the working fluid and

produces saturated steam. Steam enters in the second stage of the turbine [5] and drives the generator for electricity production. The steam at the turbine [5] outlet passes through the condenser [9] and restarts the cycle.

Cyclopentane was chosen as working fluid due to studies such as those by Peng Liu (2018) and Anandu Surendran (2020) which reports that Cyclopentane as an excellent working fluid for CRO's operating at high temperatures. The main properties of Cyclopentane are listed in Tab.Table1.

Table1: Thermophysical Properties and Environmental Data of Cyclopentane

Molecular weight [g/mol]	70,133
Evaporation Temperature at 1 atm [K]	322,4
Critical temperature [K]	511,7
Critical pressure [MPa]	4,515
GWP (1)	Too low
ODP (2)	0

(1): Global warming potential; (2): Degradation potential of the ozone layer.

The amount of energy available for waste heat recovery from exhaust gases and cooling fluid outlet were adopted according to Scaccabarozzi et al. (2018), which uses a Wartsila 46DF engine, 4 strokes of 10.3 MW of power, widely used in marine applications. The main data are shown in Tab. 2.Table 2

Table 2: Internal Combustion Engine Data

Wartsila 46DF – 4 strokes	Fuel Natural Gas; Power 10,305 kW; Efficiency 45.33 %
Exhaust Gas	Mass flow 19.00 kg/s; Calorific Rate 4,892 kW; Temperature 120 to 354 °C
Cooling Fluid outlet	Mass flow 23.16 kg/s; Calorific Rate 1,653 kW; Temperature 74 to 91 °C

It is noted that the energy potential is impacted by the large amount of exhaust gases and cooling fluid available, with mass flows of 19.00 and 23.16 kg/s respectively, rather than by the temperature values, which are in the average value of 240 °C (for the exhaust gas) and 80 °C (for the cooling fluid outlet).

2.2 Thermal cycle modeling

The thermal cycle modeling was performed in the Engineering Equation Solver (EES) software where was calculated the properties of the working fluid all thermodynamic states of thermal cycle. The modeling includes the mass, energy, entropy, and exergy balances considering physical exergy only at 298 K and 0,1 MPa as reference environment, as well as the calculation of the isentropic and exergetic efficiencies for the ORC components and the thermal cycle. Please, see as an example the following equations for the ORC from which are obtained the parameters that latter are presented and discussed in the results. In the following equations: $\dot{m}$ is the mass flow, in kg/s; *h* is the specific enthalpy, in kJ/kg; *ex* is the specific exergy (including physical and chemical portions) in kJ/kg; $\dot{Q}_{ent}$ is the inlet heat rate, in kW; $\dot{Q}_{sai}$ is the outlet heat rate, in kW; $\dot{W}$ is the net cycle power, in kW; η is the dimensional Thermal efficiency and; η_{ex} is the dimensional Exergetic efficiency:

$$\dot{Q}_{ent} = (\dot{m}_2.h_2 - \dot{m}_1.h_1) + (\dot{m}_4.h_4 - \dot{m}_3.h_3) + (\dot{m}_7.h_7 - \dot{m}_6.h_6) \quad (1)$$

$$\dot{Q}_{sai} = (\dot{m}_{10}.h_{10} - \dot{m}_{11}.h_{11}) \quad (2)$$

$$\dot{W} = (\dot{m}_7.h_7 - \dot{m}_8.h_8) + (\dot{m}_9.h_9 - \dot{m}_{10}.h_{10}) - (\dot{m}_1.h_1 - \dot{m}_{11}.h_{11}) - (\dot{m}_6.h_6 - \dot{m}_5.h_5) \quad (3)$$

$$\eta = \dot{W}/\dot{Q}_{ent} \quad (4)$$

$$\eta_{ex} = \dot{W}/(\dot{m}_{12}.(ex_{12} - ex_{13}) + \dot{m}_{14}.(ex_{14} - ex_{16})) \quad (5)$$

The thermal cycle modeling also includes the estimation of the total heat transfer surface area (*AT*) considering the sum of heat transfer surface area of the different heat exchangers of the cycle (1, 2, 3 and 9 in Fig. 1). This estimation was done by the logarithmic mean temperature difference method like was done in Moreira e Arrieta (2019).

The cost modeling was performed according to "*Chemical Process Engineering*" by Harry Silla (2003). To estimate the specific power generation cost (C), in R$/kWh, equation 6 was used:

$$C = \left(CI.\frac{F_{rec}}{H_{op}} + \varphi\right) \quad (6)$$

In Equation 6, CI is the capital investment (R$/kWh), F_{rec} is the capital recovery rate, H_{op} is the worked hours per year, φ is operation and maintenance cost (OPEX cost).

The CI is the specific capital investment cost, in R$/kW, calculate by equation 7:

$$CI = T.\left(CI_{ref}.\left(\frac{\dot{W}}{\dot{W}_{ref}}\right)^{m}\right) \quad (7)$$

In Equation 7, T is USD to R$ exchange rate; CI_{ref} it is the specific investment cost of a similar equipment taken as a reference, in US$/kW; $\dot{W}$ it is the net power generated by the ORC, in kW; $\dot{W}_{ref}$ it is the power generated by the reference ORC, in kW; m it is the evolution of the linear trend (usually lower than the unit), which for whole plants 0.6 is the usual value. The values for the variables mentioned above are shown in Tab. 3.

Table 3: General parameters for specific generation cost estimation.

Parameter	Unit	Value	Reference
T	R$/US$	5.32	Central Bank of Brazil (2021)
$H_{operação}$	h/year	8,030	-
i	% yeat	5	Brazilian Internal Revenue Service (2021)
n	years	20	-
$\dot{W}_{ref}$	kW	1,545	Surendran et al (2020)
CI_{ref}	US$/kW	808.3	Moreira et al (2019)
φ	US$/kWh	96	Diniz (2015)

We highlight the variations between the estimated price and the final price of the equipment may occur due to the simplicity of the equations employed, especially Equation 6, in which only one variable is used for the price stipulation from the reference component.

2.3 Optimization of heat recovery results

Waste heat recovery optimization aims to maximize net power generation by considering the specific investment cost for cycle construction. For this purpose, the thermodynamic modeling of the Organic Rankine Cycle of two pressure levels of Regenerative Transcritical Pressure was performed in the EES software. Subsequently, multi-objective optimization with economic analyses were performed to identify the parameters that cause the most influence in the net power and specific investment cost of the cycle. The influence of the variables used in the optimizations on the above parameters was evaluated. After selecting the parameters for optimization procedures were used genetic algorithms available in the EES for the calculations. With the help of the optimization algorithm, it was possible to find three distinct configurations for the cycle, one for maximizing the net power, another for maximizing thermal efficiency and finally one for minimizing the specific investment cost. Mathematically the optimization problems for the cycle can be formulated as MAXIMIZE net power$(\dot{W})$, MAXIMIZE thermal efficiency (η) and MINIMIZE specific investment cost (CI) subject to:

$$\left.\begin{array}{c} 78\ K \le \Delta T_{12,7} \le 101\ K \\ 10\ K \le \Delta T_{13,6} \le 38\ K \\ 20\ K \le \Delta T_{15,3} \le 24\ K \\ 4.571\ kPa \le P_7 \le 6.630\ kPa \\ \dot{\sigma}ger_i \ge 0{,}0\ \frac{kW}{K} i=1,2,3\ldots,9 \end{array}\right\} \quad (8)$$

The restrictions on the value ranges of temperature differences $\Delta T_{12,7}$, $\Delta T_{13,6}$, $\Delta T_{15,3}$, and in the range of pressure values in State 7, P_7, require that the data used be valid for the model, while the restrictions on the entropy generation $\dot{\sigma}_{ger_i}$, require that in each of the plant components (see Figure 1) the second law of thermodynamics is fulfilled. Figure 1: Representation of the chosen CRO and its T-s diagram.

3. ANALYSIS AND DISCUSSION OF RESULTS

Through modeling, simulation and parametric studies performed in the EES software, the variables of interest of the cycle that most influence their performance (net cycle power $\dot{W}$, thermal efficiency η and exergetic efficiency η_{ex}) and

cost (specific cost of electricity generation C, specific investment cost CI and total surface area of heat transfer of the exchangers AT) were identified, as well as the valid variation intervals for the developed model.

Figure 2-a shows that the relationship between $\Delta T_{15.3}$ and net cycle power is inversely proportional, indicating that the cycle will operate with maximum net cycle power when $\Delta T_{15.3}$ was minimal, the cycle requires an increase in mass flow of the working fluid to maintain a low $\Delta T_{15.3}$. On the other hand, the relationships with thermal and exergetic efficiencies are directly proportional with $\Delta T_{15.3}$, the cycle will operate with maximum values for both efficiencies when $\Delta T_{15.3}$ is maximum.

Figure 2-b shows that to keep $\Delta T_{15.3}$ minimum, a larger heat transfer surface area is required in the Preheater [1] and evaporator [2], increasing the costs of these components. The reduction in the cost caused by the increase in $\Delta T_{15.3}$ is due to the fall in the heat transfer surface area in the preheater and the evaporator.

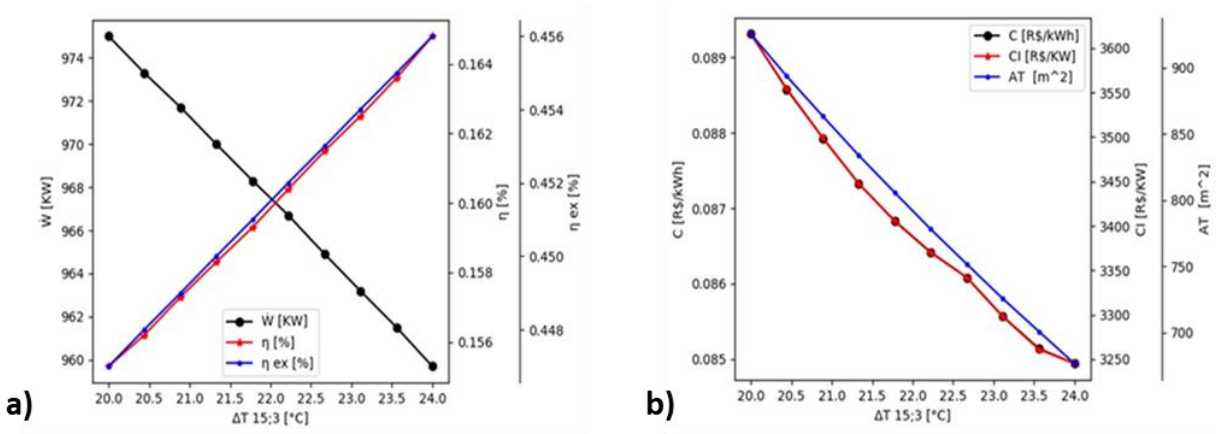

Figure 2: Variation ΔT15.3 - Low Pressure Evaporator Inlet (ΔT15.3).

Figure 3-a shows that the relationship between $\Delta T_{14.4}$ and the net cycle power is directly proportional, that is, the cycle operates with a maximum net cycle power when $\Delta T_{14.4}$ is also maximum, and that the variation in the net cycle power tends to decrease as the value of the temperature difference decreases. On the other hand, the relations between $\Delta T_{14.4}$ and thermal and exergetic efficiencies are both inversely proportional, the cycle will operate with maximum values for both efficiencies when $\Delta T_{14.4}$ is minimal.

Figure 3-b shows that an increase in heat transfer surface area provided by the increase of $\Delta T_{14.4}$ requires a larger evaporator area [2], causing an increase in cost. The rise in the specific generation cost occurs due to higher turbine cost as the net cycle power increases.

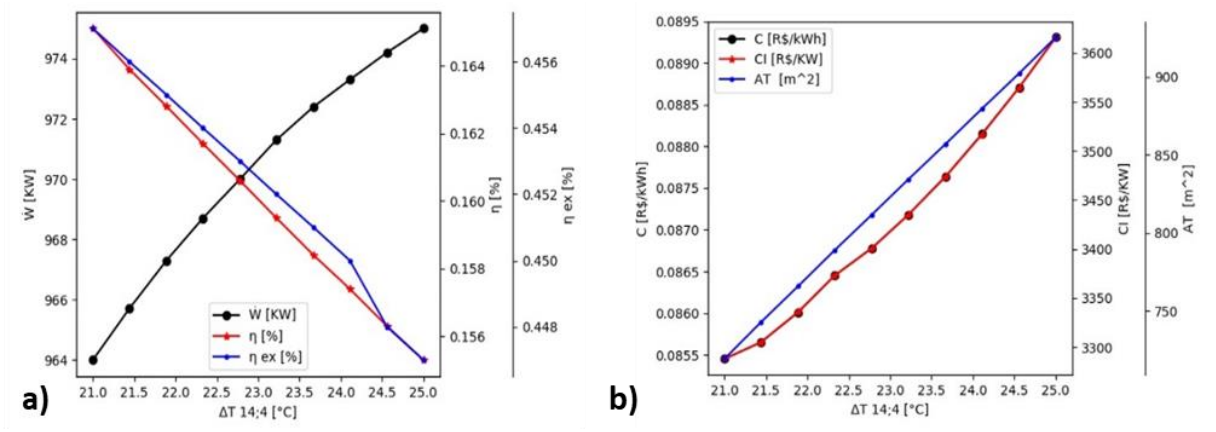

Figure 3: Influence of variation (ΔT14.4). - Low Pressure Evaporator Outlet

Figure 4-a shows that the relationship of the three variables is inversely proportional, which indicates that both net cycle power and thermal and exergetic efficiencies will be minimal when $\Delta T_{13.6}$ is maximum. The $\Delta T_{13.6}$ variation causes the most significant changes in the cycle, as there is a direct influence on the power generation of the Turbine [4], which has the highest power generation value at the minimum $\Delta T_{13.6}$. It is verified also that the sizing of the Pump [7] has a direct influence on the total energy production of the cycle.

Figure 4-b shows that with the reduction of mass flow at the inlet of high-pressure turbine, there is less heat transfer surface area in the high-pressure evaporator [3]. At this first moment, the greatest influence on the reduction of

both costs is the total heat transfer surface area of the heat exchangers, but after certain value, the cost rises due to the fall in the net cycle power.

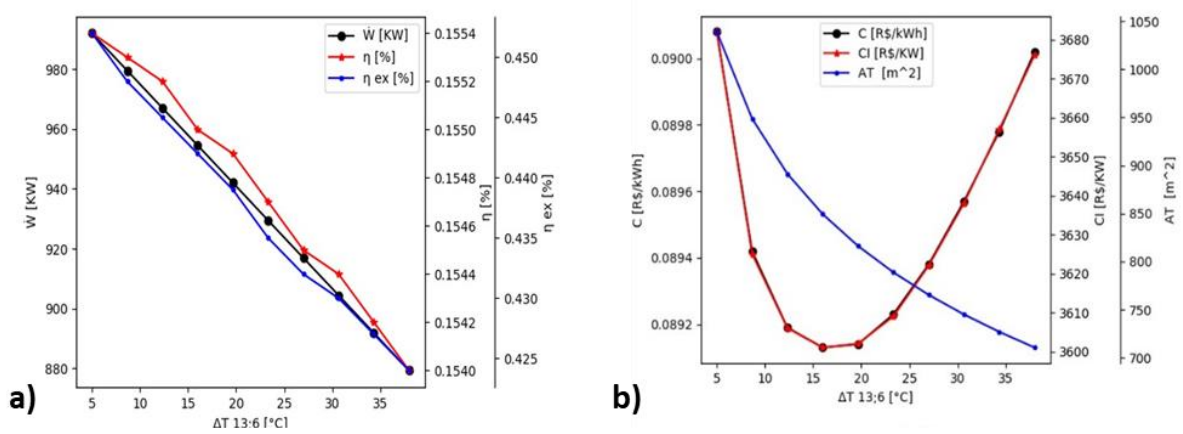

Figure 4: Variation temperature (ΔT13.6)- High Pressure Evaporator Input.

Figure 5-a indicates the maximum values for the cycle performance parameters when $\Delta T_{12.7}$ is minimal. At the evaporator output [3], the maximum values are found in the smallest temperature difference, because $\Delta T_{12.7}$ was modeled in the EES with the temperature of the fixed State 12, so this difference implies a decreasing in the temperature of the working fluid at the turbine inlet. A higher temperature at the turbine inlet has therefore a higher power generation in both turbines, causing greater thermal efficiency of the cycle.

Figure Figure 5: 5-b shows that the relationships between $\Delta T_{12.7}$ and generation costs are direct and have a convex format, while the relationship between the temperature difference between States 12 and 7 and the total heat transfer surface area of the exchangers is inversely proportional to the $\Delta T_{12.7}$ in the interval from 78 °C to 88 °C and directly proportional to the range of 88 °C to 101 °C. The behavior of the costs is directly related to $\Delta T_{12.7}$ because both as $\Delta T_{12.7}$ rise, the fall of the net cycle power, and the rise in the total heat transfer surface area.

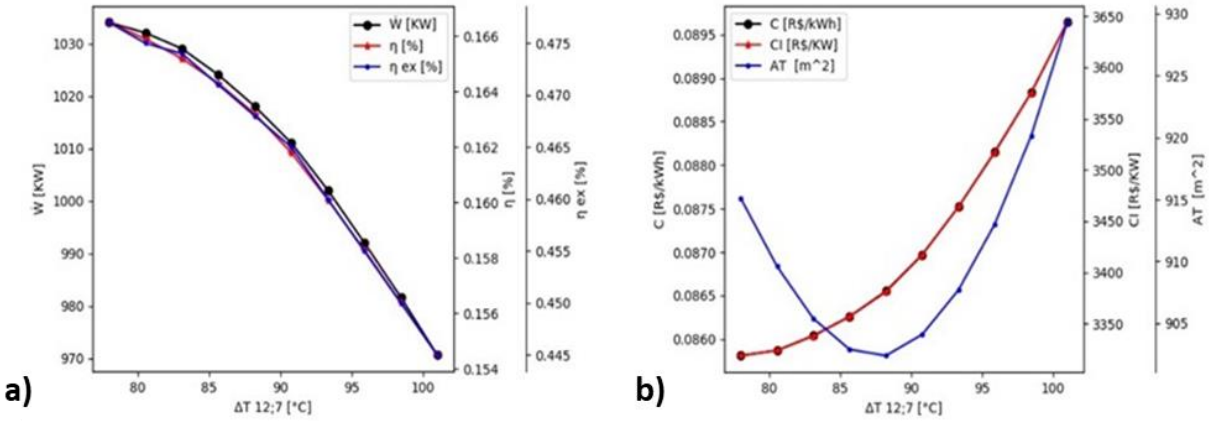

Figure 5: Variation temperature (ΔT12.7) - High Pressure Evaporator Output

Figure 6-a shows how the net cycle power, thermal efficiency and exergetic efficiency vary as a function of the pressure at the turbine inlet (State 7). It is noted that the behavior of the three variables is similar. Pressure values between ~4500 kPa and ~4750 kPa provide an irrelevant increase in net cycle power and efficiencies. An optimal point is at approximately 5000 kPa, when the maximum values of net cycle power and efficiencies are got.

FigureFigure 6: Influence of pressure variation - High Pressure Evaporator Outlet (P6-b indicates that costs increase with increased pressure, which is understood, because when adopting higher working pressures, a greater thickness of materials, pumps of greater capacity is necessary, increasing costs. Another factor that contributes to the analysis of cost behavior as a function of pressure variation in evaporator output is the influence of Component 7 (High Pressure Pump). Among all the other equipment present in the cycle, the High-Pressure Pump [7] presented the highest cost increase for higher pressure values at the output of the heat exchanger. From the cost modeling of this component, we have that the required pressure is directly proportional to the final cost obtained.

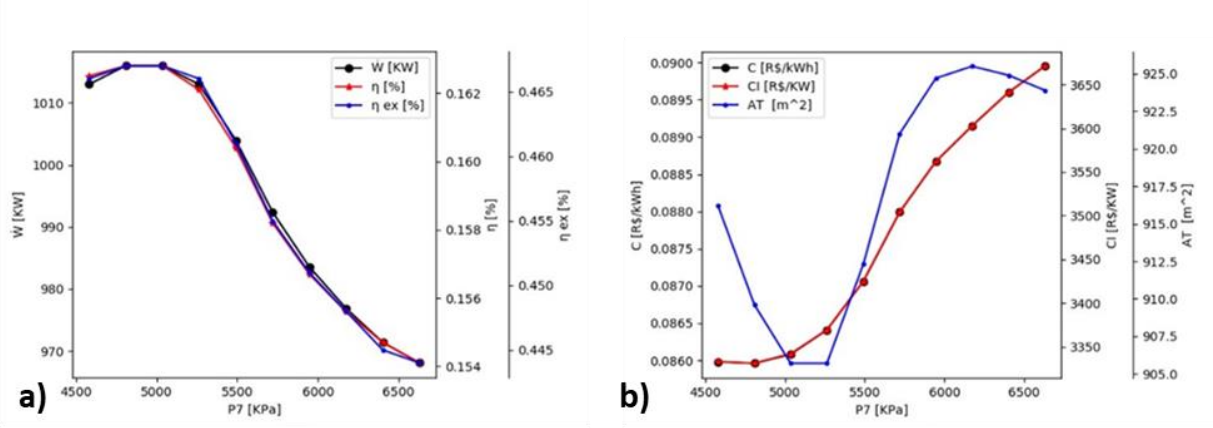

Figure 6: Influence of pressure variation - High Pressure Evaporator Outlet (P7).

Figure 7-a shows how the temperature variation in the condenser output [9], provides a sharp drop in net cycle power, thermal efficiency and exergetic efficiency. The behavior is linked to the fact that the higher the resulting temperature variation at the condenser outlet [9], the higher and closer the temperature of the working fluid will be to the temperature of the secondary heat source (Engine Cooling Fluid) circulating the PreHeater [1]. The heat exchange in the other evaporators will be lower, reducing steam generated. The loss of thermal efficiency is less.

Figure 7-b indicates as expected, the costs presented equivalent behavior, characterized by significant growth for higher values of temperature variation at the condenser output [9]. The most appropriate explanation for this behavior is the cost model adopted in cycle modeling and simulation. In it, the calculation of costs is inversely proportional to the amount of power generated, that is, the lower generation, the higher the cost without other details.

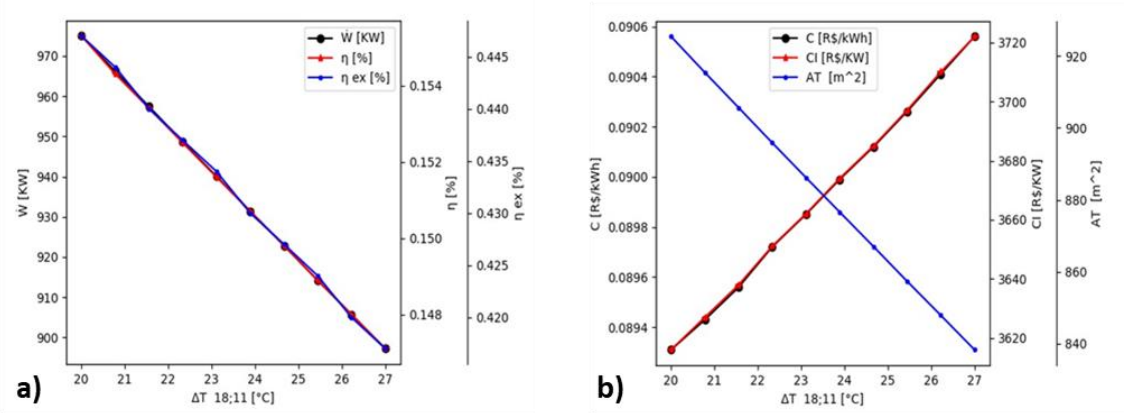

Figure 7: ΔT18.11 between FR and FT - Condenser Output (ΔT18.11).

3.1 Maximizing net power

Using the optimization procedure by genetic algorithms of the EES, we found the set of variation parameters that offer the region of maximum power considering the previously defined restrictions. Table 4 presents these values. The temperature difference (ΔT) between the MCI exhaust gas and the CRO working fluid in the Evaporator [3] (as $\Delta T_{13.6}$ rise and as $\Delta T_{12.7}$ rise, respectively), as well as the ΔT between the cooling fluid of the MCI and the working fluid of the CRO in the Evaporator [2] (as $\Delta T_{15.3}$ rise) were close to the minimum values, the pressure (P_7) at the evaporator outlet [3] was close to the maximum value. The cycle has an exergetic efficiency value elevated of 0.482. The net cycle power generated reaches 1,052 kW, with a thermal efficiency of 16.7%, and a specific investment cost of 3,391 R$/kW.

Table 4: Net Power Maximization - Optimal Point.

Variation Parameters at optimum values			Performance and Cost Parameters at the optimal point		
Description	Unit	Value	Description	Unit	Value
$\Delta T_{12.7}$	K	78.25	$\dot{W}_{liq}$	kW	1,052
$\Delta T_{13.6}$	K	5.10	η	%	16.68
$\Delta T_{15.3}$	K	20.05	C_{inv}	R$/kW	3,391
P_7	kPa	6,177			

3.2 Maximizing thermal efficiency

Through the same algorithms mentioned above, the values for the region of maximum thermal efficiency of the cycle were reached. Table 5 presents these values, performance parameters and resulting cost at the optimal point. The temperature difference between the MCI exhaust gas and the CRO working fluid at the evaporator inlet and outlet [3] ($\Delta T_{13.6}$ and $\Delta T_{12.7}$, respectively) were close to the minimum values, while the pressure (P7) at the evaporator outlet [3] and the temperature difference between the MCI cooling fluid and the CRO working fluid at the evaporator input [2] ($\Delta T_{15.3}$) are close to the maximum values. From the exergy point of view, the cycle has a reasonably high efficiency value (0.487). The net cycle power reaches 1,020 kW, with a thermal efficiency of 17.7%, and a specific investment cost of 3,026 R$/kW.

Table 5: Maximizing Thermal Efficiency - Optimal Point.

Variation Parameters at optimum values			Performance and Cost Parameters at the optimal point		
Description	Unit	Value	$\dot{W}_{liq}$	kW	1,020
$\Delta T_{12.7}$	K	78.32	η	%	17.65
$\Delta T_{13.6}$	K	8.85	C_{inv}	R$/kW	3,026
$\Delta T_{15.3}$	K	24.00			
P_7	kPa	6,027			

3.3 Minimizing investment cost

From the exergy point of view, the cycle has a reasonably high efficiency value (0.469). The net cycle power reaches 961.1 kW, with a thermal efficiency of 17.5%, and an investment cost of 2,950 R$/kW.

Table 6: Minimizing the Cost of Investment - Optimal Point.

Variation Parameters at optimum values			Performance and Cost Parameters at the optimal point		
Description	Unit	Value	$\dot{W}_{liq}$	kW	961.1
$\Delta T_{12.7}$	K	80.47	η	%	17.51
$\Delta T_{13.6}$	K	23.31	C_{inv}	R$/kW	2,950
$\Delta T_{15.3}$	K	24.00			
P_7	kPa	5,271			

3.4 Comparative analysis between optimizations

For the analysis of the three optimizations that were performed, we highlight in table 7 the main parameters. The resulting configuration of net cycle power maximization was the one with the highest specific investment cost, the lowest thermal efficiency, and the highest net cycle power. The maximization of thermal efficiency, in turn, is the one that presents the second highest net cycle power, the second lowest specific investment cost and the highest thermal efficiency. Finally, the cycle configuration that minimizes the specific investment cost presented the lowest net cycle power, the second highest thermal efficiency and the lowest specific investment cost.

Table 7: Comparison of Optimizations at the Optimal Point.

OPTIMIZATION	C_{inv} ($/kW)	$\dot{W}_{liq}$ (kW)	η (%)	$\dot{W}_{liq}/C_{inv}$
Net cycle Power Maximization	3,391	1,052	16.68	0.31
Thermal Efficiency Maximization	2,950	1,020	17.65	0.34
Specific investment cost Maximization	2,950	961.1	17.51	0.32

Thus, it is possible to affirm that the cycle configuration resulting from the maximization of thermal efficiency is the one that has the best balance between its results of net cycle power, thermal efficiency, and investment cost. It is also the optimization that has the highest ratio between net power and investment cost, which elects it as the best cycle configuration to be adopted.

4. CONCLUSION

From the minimization of electricity generation costs with small capacities CC-MCI-CRO it is possible to express the following conclusions:

- The highest net cycle power values are obtained through the temperature variation between the MCI exhaust gas and the CRO working fluid at the High-Pressure Turbine output ($\Delta T_{12.7}$) and pressure variation at the input of that same component (P_7), generating maximum powers of 1,034 kW and 1,016 kW, respectively.
- The influence on thermal efficiency is caused by the variations of ΔT (exhaust gas - working fluid) in the output of the Turbine ($\Delta T_{12.7}$) and ΔT (cooling fluid - working fluid) in the evaporator output ($\Delta T_{14.4}$), which led to percentage changes of 8% and 6% in relation to its limits found. The parameters are responsible for the highest values of thermal efficiency found, being 16.65 % and 16.51 %, respectively.
- The greatest impact on the specific investment cost was caused by the pressure at the turbine inlet (P_7), ΔT (cooling fluid - working fluid) at the evaporator inlet and outlet ($\Delta T_{15.3}$ and $\Delta T_{14.4}$) and ΔT (exhaust gas - working fluid) at the evaporator outlet ($\Delta T_{12.7}$), resulting in percentage changes of 10 % to 11 %. The lowest investment cost values are obtained through the ΔT (cooling fluid - working fluid) variation at the Evaporator inlet and outlet ($\Delta T_{15.3}$ and $\Delta T_{14.4}$), producing minimum specific investment costs of 3,245 R$/kW and 2,950 R$/kW in this order.
- By comparing the results of the three optimization operations performed, it is understood that the plant configuration that aims to maximize thermal efficiency is the one that has the best balance between its results of net cycle power, thermal efficiency, and specific investment cost, being elected as the best optimization to be adopted. The amount of electricity generated in the optimal region reaches 1,020 kW, with a thermal efficiency of 17.65 %, investment cost of 3,026 R$/kW and specific generation cost of 82.37 R$/MWh.

5. ACKNOWLEDGEMENTS

The authors would like to thank FAPEMIG, CAPES, CNPq and PUC Minas, for the support to the elaboration of this paper.

6. REFERENCES

CENTRAL BANK. Currency conversion. Available in: <https://www.bcb.gov.br/conversao>. Accessed: 17 May. 2021.

CHATZOPOULOU, Maria Anna e MARKIDES, Christos N. Thermodynamic optimisation of a high-electrical efficiency integrated internal combustion engine – Organic Rankine cycle combined heat and power system. Applied Energy, v. 226, n. May, p. 1229–1251, 2018. Disponível em: <https://doi.org/10.1016/j.apenergy.2018.06.022>.

Heywood, J.B., "Internal Combustion EngineFundamentals", McGraw-Hill Book Company (2018).

SONG, J.; SONG, Y.; GU, C. wei. Thermodynamic analysis and performance optimization of an organic rankine cycle (orc) waste heat recovery system for marine diesel engines. (2015).

Harry Silla. “Chemical Process Engineering Design & Economics” - Stevens Institute of Technology Hoboken, New Jersey, U.S.A., Marcel Dekker(2003).

IMRAN, Muhammad et al. Optimization of organic rankine cycle power systems for waste heat recovery on heavy-duty vehicles considering the performance, cost, mass and volume of the system. Energy, v. 180, p. 229–241, 2019. Disponível em: <https://doi.org/10.1016/j.energy.2019.05.091>.

LIU, Peng e SHU, Gequn e TIAN, Hua e WANG, Xuan et al. Alkanes based two-stage expansion with interheating Organic Rankine cycle for multi-waste heat recovery of truck diesel engine. Energy, v. 147, p. 337–350, 2018. Disponível em: <https://doi.org/10.1016/j.energy.2017.12.109>.

LIU, Peng e SHU, Gequn e TIAN, Hua e WANG, Xuan. Engine load effects on the energy and exergy performance of a Medium Cycle/Organic Rankine Cycle for exhaust waste heat recovery. Entropy, v. 20, n. 2, 2018.

LIU, Peng e SHU, Gequn e TIAN, Hua. How to approach optimal practical Organic Rankine cycle (OP-ORC) by con fi guration modi fi cation for diesel engine waste heat recovery. Energy, v. 174, p. 543–552, 2019. Disponível em: <https://doi.org/10.1016/j.energy.2019.03.016>.

MAHMOUDI, A. e FAZLI, M. e MORAD, M. R. A recent review of waste heat recovery by Organic Rankine Cycle. Applied Thermal Engineering, v. 143, n. July, p. 660–675, 2018. Available: <https://doi.org/10.1016/j.applthermaleng.2018.07.136>.

MAT NAWI, Z. et al. The potential of exhaust waste heat recovery (WHR) from marine diesel engines via organic rankine cycle. Energy, v. 166, p. 17–31, 2019. Disponível em: <https://doi.org/10.1016/j.energy.2018.10.064>.

MOREIRA, L. F. e ARRIETA, F.R.P. Thermal and economic assessment of organic Rankine cycle for waste heat recovery in cement plants. Renewable and Sustainable Energy Reviews, v. 114, p. 109315, 2019. Available: <https://doi.org/10.1016/j.rser.2019.109315 >.

PING, Xu et al. Prediction and optimization of power output of single screw expander in organic Rankine cycle (ORC) for diesel engine waste heat recovery. Applied Thermal Engineering, v. 182, n. 100, p. 116048, 2021. Available: <https://doi.org/10.1016/j.applthermaleng.2020.116048>.

INTERNAL REVENUE SERVICE. Long-Term Interest Rate - TJLP. Available in: <https://receita.economia.gov.br/orientacao/tributaria/pagamentos-e-parcelamentos/taxa-de-juros-de-longo-prazo-tjlp>. Accessed: May 4th. 2021

SCACCABAROZZI, Roberto et al. Comparison of working fluids and cycle optimization for heat recovery ORCs from large internal combustion engines. Energy, v. 158, p. 396–416, 2018. Disponível em: <https://doi.org/10.1016/j.energy.2018.06.017>.

SONG, Jian et al. Parametric optimisation of a combined supercritical CO 2 (S-CO 2) cycle and organic Rankine cycle (ORC) system for internal combustion engine (ICE) waste-heat recovery. Energy Conversion and Management, v. 218, n. May, p. 112999, 2020. Disponível em: <https://doi.org/10.1016/j.enconman.2020.112999>.

SURENDRAN, Anandu e SESHADRI, Satyanarayanan. Design and performance analysis of a novel Transcritical Regenerative Series Two stage Organic Rankine Cycle for dual source waste heat recovery. Energy, v. 203, p. 117800, 2020. Disponível em: <https://doi.org/10.1016/j.energy.2020.117800>.

TIAN, Yaming et al. Development and validation of a single-piston free piston expander-linear generator for a small-scale organic Rankine cycle. Energy, v. 161, p. 809–820, 2018. Disponível em: <https://doi.org/10.1016/j.energy.2018.07.192>.

XU, Bin et al. A comparative analysis of real-time power optimization for organic Rankine cycle waste heat recovery systems. Applied Thermal Engineering, v. 164, n. August 2019, p. 114442, 2020. Available: <https://doi.org/10.1016/j.applthermaleng.2019.114442>.

YANG, Fubin et al. Artificial neural network (ANN) based prediction and optimization of an organic Rankine cycle (ORC) for diesel engine waste heat recovery. Energy Conversion and Management, v. 164, n. March, p. 15–26, 2018. Available: <https://doi.org/10.1016/j.enconman.2018.02.062>.

YANG, Min Hsiung. Payback period investigation of the organic Rankine cycle with mixed working fluids to recover waste heat from the exhaust gas of a large marine diesel engine. Energy Conversion and Management, v. 162, n. 142, p. 189–202, 2018. Available: <https://doi.org/10.1016/j.enconman.2018.02.032>.

ZHAO, Rui et al. Integrated simulation and control strategy of the diesel engine–organic Rankine cycle (ORC) combined system. Energy Conversion and Management, v. 156, n. 100, p. 639–654, 2018. Available: <https://doi.org/10.1016/j.enconman.2017.11.078>.

7. RESPONSIBILITY NOTICE

The authors are the only responsible for the printed material included in this paper.